Research Article

Journal of Environmental Nanotechnology

Investigation of Screen Mesh Wick Heat Conduit using Aluminum Oxide Nanofluid with Deionized Water as the Base Working Fluid

C. Senthilkumar[1*], J. Yogaraja[2], T. Srinivasa Rao[3] and L. Karthick[4]

[1]Department of Mechanical Engineering, SNS College of Technology, Saravanampatti, Coimbatore, TN, India
[2]Department of Automobile Engineering, Hindusthan College of Engineering and Technology, Coimbatore, TN, India
[3]Department of Engineering Mathematics, Koneru Lakshmaiah Education Foundation, Vaddeswaram, AP, India
[4]Department of Mechanical Engineering, Hindusthan College of Engineering and Technology, Coimbatore, TN, India
Received: 08.08.2024 Accepted: 28.11.2024 Published: 30.12.2024
*senthilkumarsnsct@gmail.com

ABSTRACT

This investigation was focused on analyzing heat conduits' heat energy transport characteristics using deionized water and aluminum oxide nanofluid as the working media. By varying the angle of inclination of the heat conduit from 0 to 90° and adjusting the heat load from 40 to 200W, comparisons were made between deionized water (base fluid) and water-soluble Al_2O_3 nanofluid. Performance evaluation parameters included thermal efficiency, heat resistance, and heat transfer coefficient. Compared to the base fluid, the use of the nanofluid improved the thermal performance of the screen mesh wick heat conduit, as evidenced by the experimental findings. The heat transfer coefficient increased from 5.68 to 21.7% due to the enhanced heat load and changed orientation due to gravitational effects. Furthermore, the overall thermal resistance decreased from 6.85 to 17.7% with the rise in heat load and orientation. Incorporating nanoparticles and altering the orientation not only expanded the operational range but also enhanced the overall thermal efficiency of the heat conduit when compared to the base fluid.

Keywords: Screen mesh; Wick; DI water; Aluminum oxide; Heat transfer.

1. INTRODUCTION

The most efficient method for transferring heat passively involves the utilization of heat conduits. These conduits possess exceptional thermal conductivity, enabling the smooth transfer of heat while ensuring a consistent temperature balance between the heated and cooled elements. Heat conduits can transport substantial heat quantities across extensive distances as stationary thermal transfer instruments through phase-change mechanisms and vapor diffusion. At the core of a heat conduit lies an evacuated tube, partially filled with a working substance that can transition between fluid and gas forms.

Pak and Cho (1998) conducted innovative experiments involving nanoparticles (specifically oxide) suspended in water within a circular conduit. The utilization of dispersed fluids as an operational substance suggests the importance of selecting particles with high thermal conductivity and larger dimensions to enhance the heat transfer coefficient. Do and Jang, (2010) experimented to produce a heat conduit featuring a rectangular grooved wick and utilizing deionized (DI) water-based Al_2O_3 nanofluids as the operational fluid. The findings indicated a reduction in the thermal resistance of the heat conduit with an increase in the nanoparticles' size. Kumaresan *et al.* (2014) investigated the impact of surfactant-free copper oxide nanoparticles that were dispersed in the DI water with copper sintered wick heat pipe. The results revealed a significant decrease in thermal resistance by 66.1%, accompanied by improvements in heat transfer coefficient (HTC) by 29.3% and thermal conductivity by 63.45%. Ma *et al.* (2006) examined the performance of a nanofluid oscillating heat conduit utilizing diamond nanofluid as the working medium. When subjected to a power input of 80 W, the nanofluid exhibited a notable decrease in the temperature gradient between the evaporator and condenser sections, reducing between 40.9°C to 24.3°C. These findings underscore the superior performance compared to the conventional cooling techniques. Shukla *et al.* (2012) demonstrated a quantitative improvement in the heat transfer coefficient when the heat conduit was charged with a nanofluid. This enhancement was attributed to the superior thermal conductivity and increased surface area provided by copper nanoparticles, which facilitated more efficient heat transfer. Park and Ma (2007) fabricated and tested an oscillating heat conduit with no turns. The oscillating motions in this

well-balanced heat pipe were found to be very irregular, in contrast to the regular oscillating motions observed in the oscillating heat conduit. In this study, the optimal heat transfer performance was achieved when the heat conduit was charged with nanofluid at a 50% filling ratio.

Kim *et al.* (2007) examined the characteristics of critical heat flux by conducting experiments with nanofluids containing different concentrations of Al_2O_3 or TiO_2 nanoparticles. These experiments were performed and tested with a 0.2 mm diameter cylindrical Ni–Cr wire under atmospheric pressure. The results indicated that the heat flux of nanofluids was significantly higher than that of base fluid. Moraveji and Razvarz (2012) studied the thermal performance enhancement of a grooved heat conduit by utilizing Al_2O_3 nanofluid as the working fluid. The heat conduit, featuring a 1 mm wick-sintered circular design, was experimentally tested. The findings indicated that charging the heat conduit with Al_2O_3 nanofluid resulted in improved thermal performance, characterized by a reduction in both thermal resistance and change in the wall temperature. Razvarz and Jafari (2018) examined the impact of curvature, working fluids, and inclination angles on the thermal efficiency of thermosyphon and heat conduit. The experiments were conducted with different inclination angles of 30, 60, and 90° (vertical), and repeated for consistency. The results indicated that a tilt angle of 60° yielded superior thermal performance. Additionally, at a nanoparticle concentration of 1% by volume, the Al_2O_3/water nanofluid significantly enhanced the heat transfer. Senthilkumar *et al.* (2012) experimented with a heat conduit with CuO as the working fluid. The CuO nanoparticles prepared in the ultrasonic homogenizer with an average size of 40 nm (diameter) were dispersed uniformly in the base fluid, with a nanoparticle concentration of 100 mg/l. CuO nanofluid exhibited higher thermal efficiency and significantly lower thermal resistance when compared to the base fluid. Bharathiraja *et al.* (2024) evaluated the performance of a horizontal micro-grooved heat conduit using CuO nanofluid as the working medium. The average diameter of CuO nanoparticles was 50 nm, and the particle concentration was from 0.5 to 2.0 wt. %. The results indicated that CuO nanofluid enhanced the thermal performance of the heat conduit, with the optimal mass concentration for achieving the greatest heat transfer improvement, estimated to be 1.0 wt. %. Senthilkumar *et al*. (2020) developed a wickless heat pipe and tested it with different heat inputs from 50 to 250 W, and the thermal resistance of the heat pipe was examined with various inclination angles: 0°, 45°, and 90°, relative to the horizontal position. The results showed that at a heat flux of 10 kW/m², and with an inclination angle of 45°, the condenser and evaporator heat transfer coefficients of the wickless heat pipe were approximately 11% and 25% higher, respectively, when compared to the uncoated heat pipe.

Kang *et al.* (2006) examined the improvement in heat conduit performance achieved by using silver nanofluid as the working fluid. Specifically, deionized water mixed with silver nanoparticles of 10 nm and 35 nm was tested inside a heat conduit with dimensions of 211 µm wide and 217 µm deep. The thermal resistance values for two nanoparticle sizes using deionized water were obtained; the maximum reductions observed were 50% for 10 nm particles and 80% for 35 nm particles, indicating that the thermal resistance of the grooved heat pipe was influenced by the size of the nanoparticles. Naphon *et al.* (2008) developed a heat conduit with an outer diameter of 0.015 m and a length of 0.6 m. The performance of the heat conduit was tested with deionized water, alcohol, and nanofluids. The titanium nanoparticles with a diameter of 21 nm were used in this study, and the alcohol-nanoparticle mixtures were prepared using an ultrasonic homogenizer. The thermal efficiency was improved by 10.0%, 15.0%, and 20.0% for the 0.1%, 0.5%, and 1.0% Ti nanofluid concentrations, respectively, compared to the deionized water case. Manay *et al.* (2019) attempted to identify the maximum particle volume fraction limits for improving heat transfer performance in the TiO_2 nanofluids within a microchannel heat conduit. The effects of the Reynolds number and various particle volume fractions (0.25, 0.5, 1.0, 1.5, and 2.0) were analyzed at a constant microchannel height of 200 µm to assess their impact on the thermal performance of the microchannel heat sink. The results indicated that TiO_2 particles enhance the heat transfer with a volume fraction of 1.5 vol. %, but higher pressure drops in the microchannel heat conduit result in increased pumping power. Karthick *et al.* (2024) studied the physical properties, pressure drops, and heat transfer rates of SiO_2 nanofluids in a heat conduit. The results showed significant differences in the physical properties between SiO_2 nanofluids and base fluid. For low-volume-concentration nanofluids, the friction factor increased slightly in the laminar flow and appeared to be nearly independent of the Reynolds number in turbulent flow. The impact of combined heat transfer enhancement was considerably superior to that of individual heat transfer enhancement alone. Celata *et al.* (2013) conducted an experiment with various nanofluids, including TiO_2 and SiC nanoparticles at different concentrations, and analyzed them in detail against water. The experimental data indicated a strong dependence on the parameters used, with both the nanofluid and water data aligning closely with the calculated values.

Vidhya *et al.* (2021) studied the heat transfer performance of a heat conduit by using a hybrid of Al_2O_3 and SiO_2 nanoparticles in a W/EG binary mixture. The results indicated that both the heat transfer capacity and the volume concentration of the hybrid nanofluid increased with the heat input power. Bumataria and Chavda (2022) developed a heat conduit with a copper screen mesh wick; nanoparticles (Al_2O_3, CuO,and ZnO)

were added to the base fluid at a concentration of 1.0 wt. %. The result reported that, at a 60° angle, CuO nanofluids had greater thermal enhancement than other working fluids. The reduction in thermal resistance for CuO was 27.51%, 36.21%, and 57.58% less than that of Al_2O_3, ZnO, and the base fluid, respectively. Additionally, enhancing the heat load resulted in a delay in thermal improvement. Mohanraj *et al.* (2021) observed the performance improvement in solar still using nanofluids. Karthick *et al*. (2022) and Bharathiraja *et al.* (2024) analyzed different refrigerants and nanofluids to improve the performance of turbines.

Based on the above literature review, in this study, a novel investigation was introduced into the thermal performance of heat conduits, specifically focusing on the use of Deionized (DI) water and aluminum oxide nanofluid as working fluids. The research highlighted how varying the inclination angle and heat load influenced the thermal characteristics of the conduit. The significant finding was that the use of Al_2O_3 nanofluid, particularly with nanoparticles of 85 nm diameter, led to noticeable enhancements in heat transfer efficiency. By optimizing the orientation and heat load, the study reported a substantial improvement in the HTC and a reduction in thermal resistance, showcasing the potential of nanofluids to improve thermal management systems beyond the capabilities of conventional fluids.

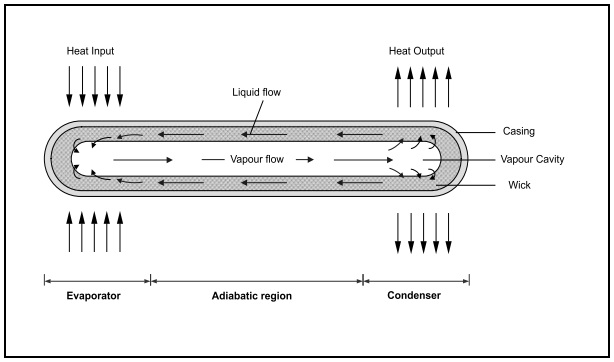

Fig. 1: Structure of Thermosyphon and Wicked heat conduits

Heat conduits exhibit efficient thermal superconductor characteristics by facilitating a high rate of heat transfer, rendering the system applicable to a diverse array of uses. The initiation of a novel cycle stands as a fundamental operation within this context. Positioned at the base of the conduit was the working fluid, which can undergo evaporation through the introduction of a heat source. As a result of the disparity in densities between the vapor and the fluid, the vapor could access the condenser segment. Upon condensation of the vapor, latent heat was discharged due to the temperature variance between the walls, thus enabling the fluid to revert to the liquid pool of the evaporator by either gravity (thermosyphon) or a capillary wicking structure (wicked heat conduits), as illustrated in Fig. 1. Incorporating various geometrical parameters sourced from extensive literature reviews, heat conduits were employed in this research work with a nanoparticle size of 85 nm.

2. PREPARATION AND CHARACTERIZATION OF AL_2O_3 NANOFLUIDS

In this study, deionized water served as the foundational fluid, with the predominant nanoparticles being Al_2O_3 nanoparticles (Al_2O_3NPs), characterized by a size of 85nm based on SEM evaluation. The Al_2O_3NPs were introduced into the pristine water. The SEM images illustrated in Fig.2, confirmed the existence of Al_2O_3nanoparticles alongside Al_2O_3powder. The resultant nanofluid consisted of 99.0% pure Al_2O_3, featuring an average particle size of 85nm that was previously dispersed in water. Employing an ultrasonic homogenizer, the nanoparticles were effectively blended with pure water at volume fractions of 0% and 1%. Utilization of bath-type sonicators was essential to prevent agglomeration during the nanofluid synthesis process. The fundamental properties of deionized water, namely density, viscosity, thermal conductivity, and specific heat, were 983.3 kg/m^3, 4.67 × 10^{-4}Pa-s, 0.682W/m K, and 4.183kJ/kg K, respectively.

Fig. 2: SEM image of Aluminum oxide powder (85 nm nanoparticles)

Table 1. Requirements of Heat Conduit

Heat conduit	Copper
Wick	Copper (Screen mesh)
Pipe length (Total)	400 mm
Evaporator region	100 mm
Adiabatic region	200 mm
Condenser region	100 mm
Pipe diameter (Outside)	20.5x 10^{-3} m
Pipe diameter (Inside)	17.5 x 10^{-3} m
Working medium	Water and Al_2O_3
Particle size	85nm
Mesh size per inch	60
Number of layers	4
Mesh wire diameter	8 x 10^{-3} m
Mesh size	100 mesh/in.

2.1 Nanofluid Properties

The nanofluid density was determined using,

$$\rho_{nf} = \Phi\ \rho_{nf} + (1-\Phi)\ \rho_{bf} \quad \ldots (1)$$

The specific heat of nanofluid was ascertained through the equation:

$$(\rho C_p)_{nf} = \Phi(\rho C_p)p + (1-\Phi)(\rho C_p)_{bf} \quad \ldots (2)$$

In this context, ρ represents the density of the fluid, C_p denotes its specific heat, while bf and nf respectively refer to the base fluid and nanofluid. The assessment of thermal conductivity was executed using the KD2 Pro Thermal Properties Analyzer from Decagon Devices, Inc., which employed transient hot wire techniques. The precision of measurement with this instrument is estimated to be below 5%. The introduction of Al_2O_3nanoparticles into the nanofluid resulted in a proportional increase in its thermal conductivity. The determination of nanofluid dynamic viscosity was carried out using a Brookfield Viscometer with an accuracy of 1%; the viscosity of nanofluids is inherently linked to their concentration.

2.2 Experimental Setup

Two ends of a 0.4 m long heat conduit with a 0.0205 m outer diameter copper tube were sealed. One gate valve is equipped with a filling line for charging the working fluid. The inner tube had a four-layer 100-mesh copper screen, which was kept in place by a spring arrangement. To eliminate the non-condensable within the copper tube, it was evacuated to 28 mbar and heated to 400°C, which it was able to sustain for roughly 6 hours. The accurate quantity of working fluid (17 ml, adequate to fully saturate the wick) was introduced via a capillary tube by adjusting the vacuum valve. Subsequently, the capillary tube underwent crimping. The initial temperature of the water is controlled and established at 20.5°C by utilizing a thermostatic bath with a flow rate of 1.7 liters per minute to sustain an appropriate operational temperature as the heat input rises. Experiments with varied heat fluxes were carried out in three distinct orientations. The orientation of the heat conduit inclination angles is depicted in Fig. 5. The temperature in the laboratory is kept at 25 + 1°C. The evaporator, adiabatic, and condenser parts of the heat conduit under investigation were made up of three pieces.

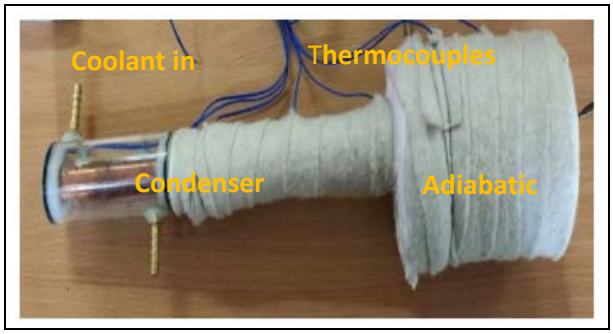

Fig. 3: Fabricated heat conduit

Fig. 4: Heat conduit with wick material

3. TEST PROCEDURE

Fig. 5 depicts the experimental setup, which comprises a 1000 W resistance heater, a wattmeter, and an autotransformer to deliver electricity to the heaters. Only a PC-based data gathering device was used to capture the temperature readings at various places along the heat conduits and it was measured by K-type thermocouples concerning the 6 different locations (6 numbers). Fig. 5 shows the configurations of temperature sensors that measure the cooling water intake and exit temperatures by K-type thermocouples (2 numbers). The cooling water volume was measured in a steady-state condition.

The activation of the power supply occurred after the insulation of the heater and adiabatic section using glass wool measuring 10 mm in thickness. The adjustable transformer modulated the thermal input within a range of 40 to 200 W. The data acquisition

system oversaw the monitoring of both the cooling water inlet and outlet, in addition to the heat transfer passage. Upon achieving a stable condition in the heat transfer passage, the flow rate of water through the condenser was quantified.

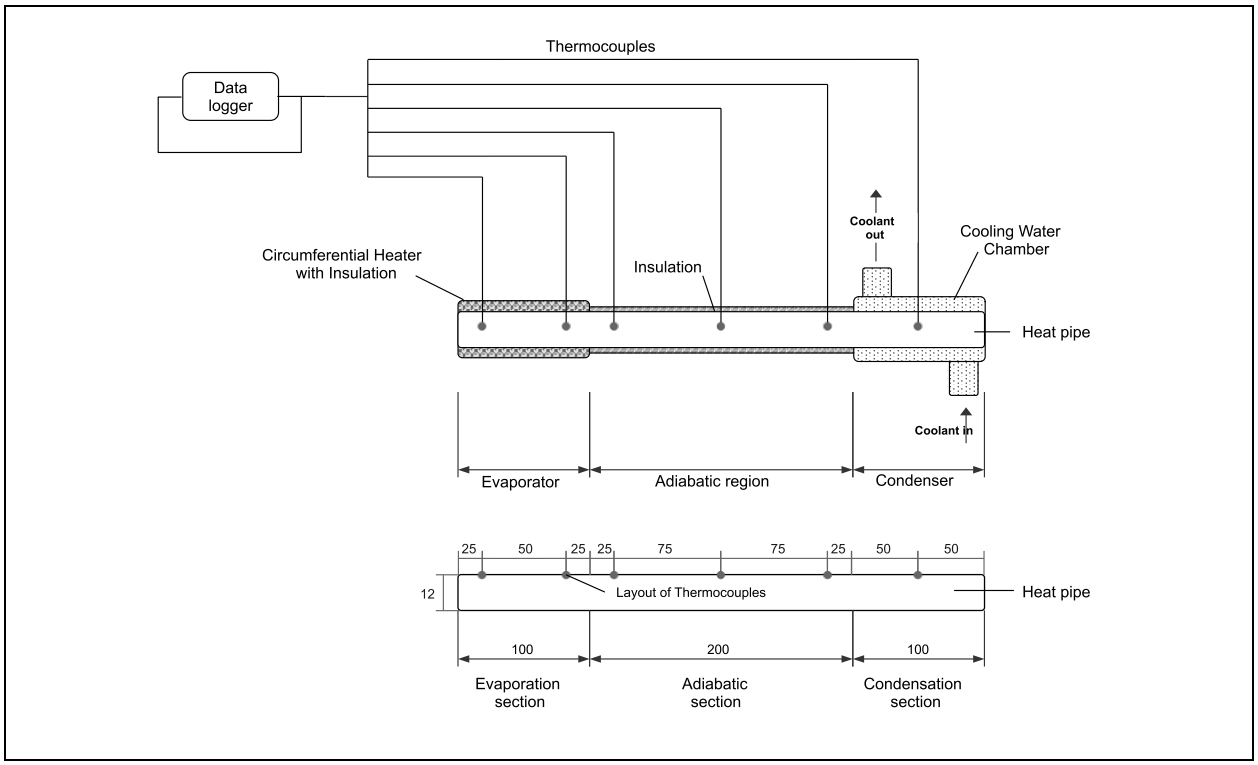

Fig. 5: Layout of the experimental setup

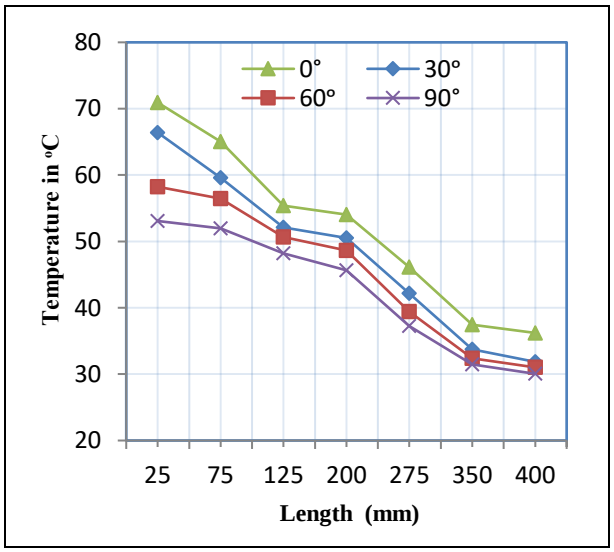

Fig. 6: Temperature variations with axial length at 0 to 90 °C

When the switch was activated, the evaporator received heat from the heater. A time period ofapproximately40–45minutes was required for the experimental conditions to stabilize. Measurements of temperatures and various system parameters were taken, once the system reached a stable state during each stage. Subsequently, the power level was adjusted upwards, and this cycle was repeated until the thermocouple in the evaporator detected an abrupt temperature rise, positioned distantly from the condenser, indicating the absence of liquid in the system. As the evaporator and condenser became completely devoid of liquid, the temperature difference between them became more pronounced. Thermocouples were affixed to the evaporator, adiabatic region, and condenser sections, numbering two, three, and one respectively, along the walls of the heat transfer conduit. The impact of thermal effectiveness in varying orientations utilizing nanofluid can be explored by monitoring and evaluating the proportion of heat removed by the condenser from the coolant in comparison to the heat supplied by the evaporator, in conjunction with the input of heat and orientation of the heat transfer conduit.

4. RESULTS AND DISCUSSION

4.1 Effect of Average Temperature Variation and Length of the Heat Conduit on Different Angles

The impact of the heat conduit's (HC) geometry and the characteristics of the base fluid on its performance was significant. Evaluating the temperature profile along the heat conduit, with different inclination angles in the evaporator and condenser, involved considering various fluid conditions in the current

experiments. Fig. 6 illustrates the relationship between the wall surface temperature and the length of the heat conduit with multiple power inputs, inclination angles, and compositions of Al_2O_3nanofluid. The temperature increased with higher power inputs, as depicted in these graphical representations. The utilization of charged nanofluid as the working medium in a heat conduit resulted in a lower wall temperature compared to standard DI water, thereby improving overall performance. Additionally, an increase in the nanofluid dispersion led to a decrease in wall temperature. The temperature distribution variations in the evaporator section to the condenser section, as shown in Fig. 6 serve as a basis for discussing the impact of different inclination angles. A temperature contrast of 7.2 percent between the base fluid and Al_2O_3nanofluid was observed in the horizontal orientation, while it was 5.1 percent at a 90-degree inclination.

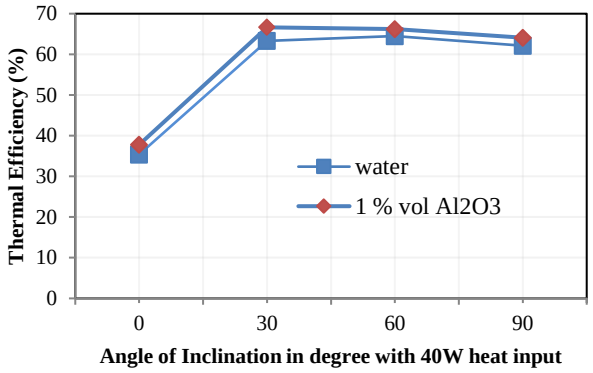

Fig. 7 (a): Efficiency vs. Inclination angle at 40 W

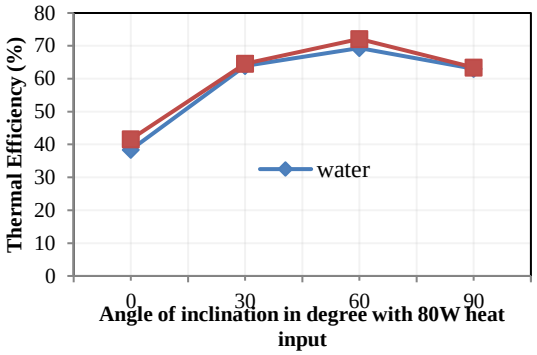

Fig.7 (b): Efficiency vs. Inclination angles at 80 W

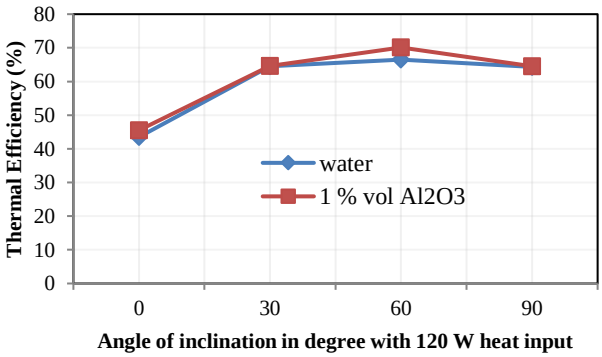

Fig.7 (c): Efficiency vs. Inclination angles at 120 W

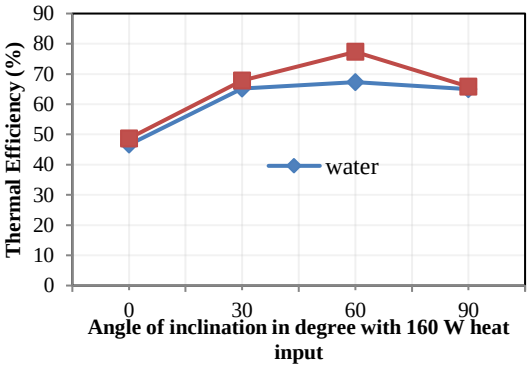

Fig.7 (d): Efficiency vs. Inclinations angles at 160 W

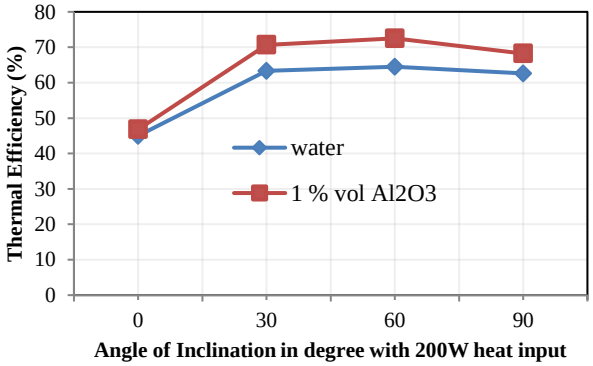

Fig.7 (e): Efficiency vs. Inclination angles at 200 W

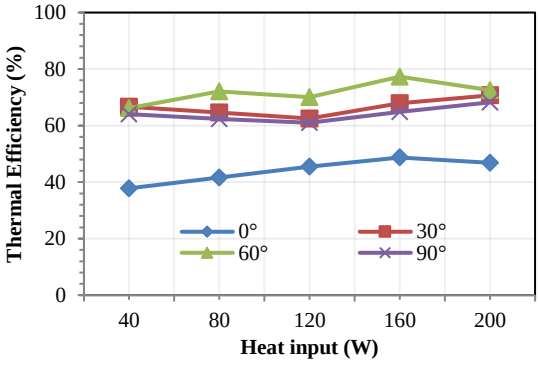

Fig.7 (f): Efficiency vs. Heat input with different angles for 1 % vol. Al_2O_3

4.2 Significance of Orientation and Heat Load on Efficiency

The thermal performance of a heat conduit involves dividing the cooling rate capacity of the condenser fluid in the condenser region by the input power at the evaporator region. Variations in heat conduit thermal efficiency concerning heat conduit orientation are depicted in Figures 7 (a-f). The thermal efficiency of the heat conduit exhibited an increasing trend with the orientation angle, reaching a peak at 60° for both DI water and Al_2O_3 nanofluid. This trend is directly related to the horizontal position of the heat conduit, as illustrated in all figures.

$\Delta T = (T_{bf}-T_{nf})$ was decreasing from the horizontal position to the perpendicular position.

The temperature of the working substance increases, enabling the condensate section to transfer a greater amount of heat. The evaporator and condenser region working medium was influenced by the wick's capillary action and the microgravity gradient.

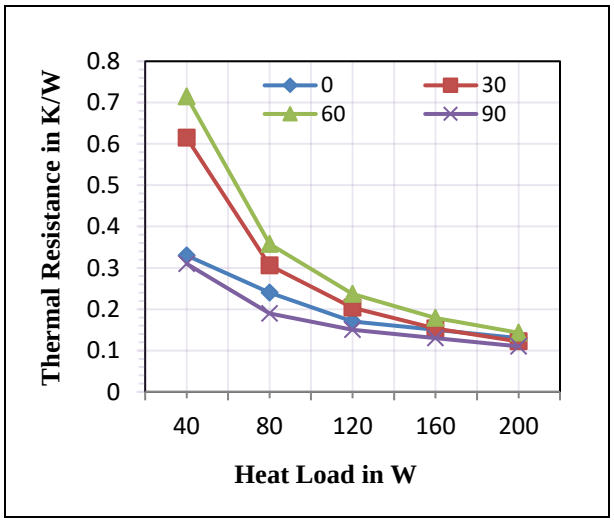

Fig. 8: Thermal resistance vs. Heat load in various tilt angles

When the heat conduit angle of inclination exceeded 60°, the thermal efficiency started decreasing. The rate of formation of liquid film inside the condenser was faster because of higher thermal resistance. In addition to their higher thermal conductivity and heat capacity, the alumina nanoparticles present in the heat conduit had a substantial impact on heat transfer enhancement. As a result, the thermal efficiency of the heat conduit with Al_2O_3nanofluids was enhanced by 5 to 10%, compared to the base working fluid. Nanofluids have a higher thermal conductivity as their volume concentrations rise. Nanoparticles have substantially improved the distribution and transmission mechanism of the base liquid (Karthick *et. al.* 2024). Smaller particles have a larger surface area for colliding particles, thereby increasing the frequency of reaction and improving the catalytic and responder properties.

4.3 Thermal Resistance

Fig. 8 depicts the heat resistance of a heat conduit filled with Al_2O_3 nanofluid. The following equation was used to evaluate the heat resistance (R) of a heat conduit:

$$R = \frac{T_{evp}-T_{cond}}{Q_{heater}} \quad \ldots (3)$$

The average mean temperature of the evaporator and condenser, denoted as T_{evp} and T_{cond} respectively, are considered along with the heat input to the heat conduit, Q_{heater}. It indicated that the heat resistance of the heat conduit reduced with an increase in the angle of inclination and heat input, as illustrated in Figures 8 and 9. Particularly, at low heat input levels, both heat conduits exhibited notable thermal resistance because of the presence of a relatively dense liquid coating in the evaporator section. However, with a rise in heat input, the thermal resistance gradually declined. Notably, nanofluids consistently demonstrated a lower resistance to heat flow compared to DI water, with the difference ranging from 5 to 10%.

The thermo-physical characteristics of nanofluids, in addition to the development of a thin, permeable layer of coating created by nanoparticles within the evaporation region, play a role in the higher heat transfer within a heat conduit utilizing nanofluids (Vidhya *et al.* 2021). Through the reduction of contact angle and the augmentation of surface roughness, the nanoparticle coating layer promotes mixing, augments critical heat flux, and significantly reduces the resistance to heat transfer of the nanofluid heat conduit (Moraveji and Razvarz, 2012).

The thermal resistance variations of heat conduits crafted from DI water and 1% Al_2O_3nanofluid were demonstrated. In instances of minimal heat load, the thermal resistance of the heat conduits remains elevated, irrespective of the fluid employed. Significant surface tension was observed at the solid-liquid interfaces under conditions of low heat flow or temperature; however, this phenomenon diminished with escalating heat flux or temperature. For moderate heat loads, the liquid layer's film thickness was also high. Even though the film thickness decreased as the heat input increased, this resulted in a significant reduction in the heat resistance. As the thermal load increased, there was a reduction in heat resistance to differing extents of inclination. Across the spectrum of 0, 30, 60, and 90°, the thermal resistance diminished as the angle of inclination increased. Adding Al_2O_3nanoparticles led to a significant decrease in thermal resistance. A thin coating layer was created on the wick surface by the flow of nanofluid, enhancing

capillary action, and consequently increasing the rate of heat transfer.

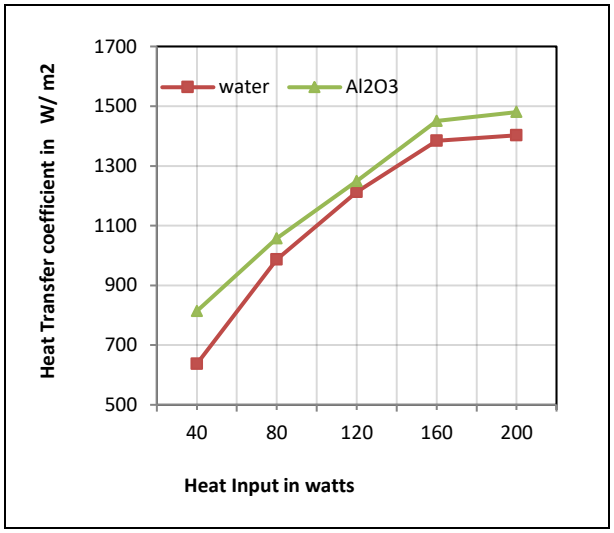

Fig. 9 (a): HTC vs. Heat input at 30°

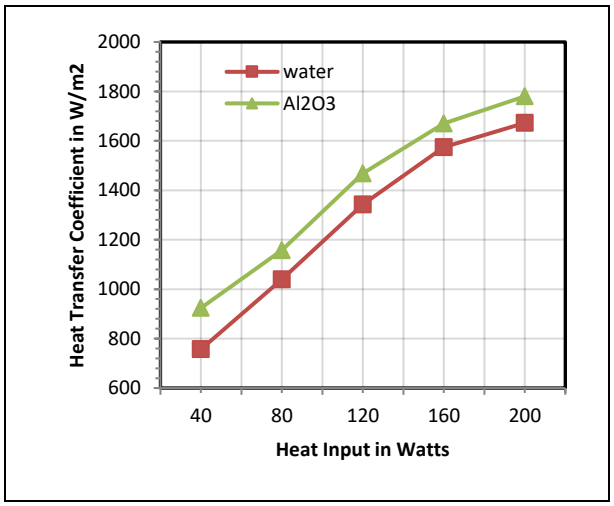

Fig. 9 (b): HTC vs. Heat input at 60°

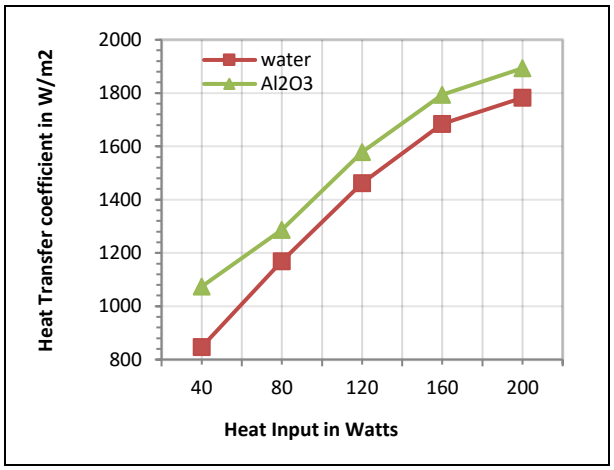

Fig. 9 (c): HTC vs. Heat input at 90°

4.4 Effects of Tilt Angle and Heat Input on HTC

Figures 9(a-c) illustrate the comparison of HTC enhancement among nanofluid and base fluid with different inclination angles. The HTC improved when the nanofluid was being used as a working medium, depending on the inclination angle and the heat load. This improvement was high at 90° inclination and low for the rest of the angles due to its poor capillary action during testing. Furthermore, heat transfer coefficients increased by 5.68 to 21.7% over the heat conduit with nanofluid as a medium for almost all heat loads and orientations. It may be due to the wettability angle between the surface and fluid interaction which revealed that the nanofluids were most suitable compared to the base working fluid. The HTC of heat conduit was evaluated by the following equation:

$$h = \frac{Q}{2\pi rl} \cdot \frac{1}{\bar{T}_e - \bar{T}_v} = \frac{q}{\Delta T} \quad \ldots (4)$$

The temperature in the condenser section and evaporator section was considered to be the average adiabatic temperature of the heat pump. Fig. 10 showcases the temperature changes on the surface of the heat conduit along its length. The Al_2O_3 nanofluid exhibited heat flux densities of 7.76 kW/m² at a concentration of 1% by volume. A volume fraction of 1.0 vol.% of Al_2O_3 nanofluid was utilized in the research, with comparisons drawn to the results of deionized water in the heat conduit. The surface temperature was higher compared to the condenser section due to the proximity of the evaporator and the electric heater around it. Consequently, the heat transfer took place from the surface of the evaporator to the core of the vapor.

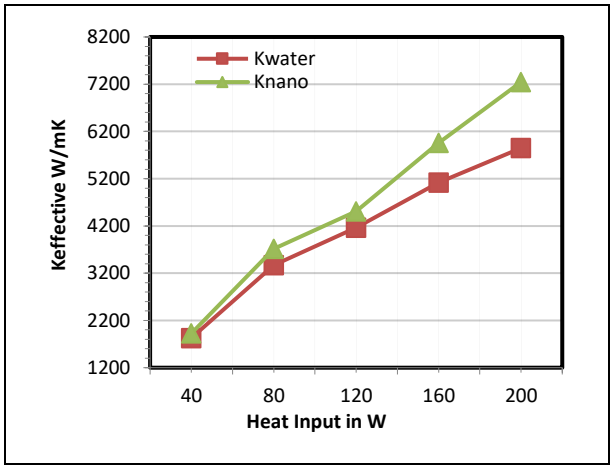

Fig. 10: Effective thermal conductivity of HC at 90° inclination

The surface temperature of the condenser was lowered when compared to that of the evaporator because of the direct contact between the condenser surface and the cooling water. Additionally, the temperature between

the evaporator and condenser reduced notably with the addition of Al_2O_3nanoparticles in the base fluid. Specifically, a maximum temperature differential of 9.1 ℃was noted at the evaporator segment of the heat conduit, which decreased to 3.8 ℃ for a 1 wt. % concentration of Al_2O_3 nanofluid heat conduit with an inclination angle of 60°.

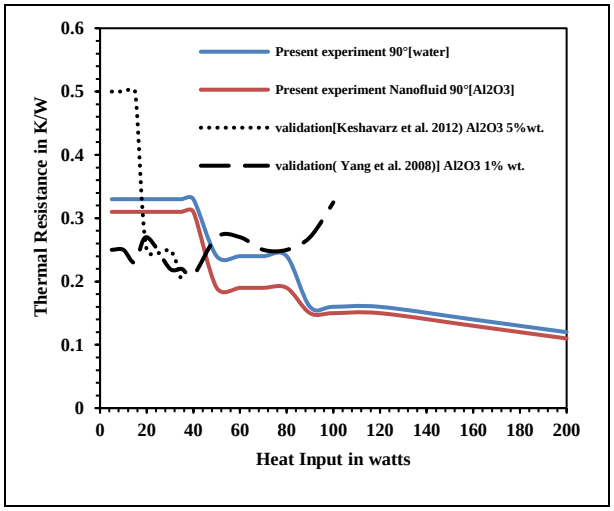

Fig. 11: Validation of thermal resistance with a few experiments in HC at 90° inclination

4.5 Effective Thermal Conductivity

Effective thermal conductivity is another performance parameter, comparable to heat conduit efficiency, which may be used to assess and compare heat conduits with multiple genres. The contact of the working fluid with the metal configuration transfers heat through the condenser section. It was found that for the effective thermal conductivity a rise in trend was noticed from the beginning of the heat input itself and it showed a major rise with higher heat input from 100 to 200W. The enhancement in effective thermal conductivity was attributed to the active Al_2O_3 nanofluid serving as the working medium, coupled with its interaction with the wick mesh surface. This interaction facilitated capillary action, driving the working medium from the evaporator to the condenser. A minor variation in the effective thermal conductivity was observed due to the boiling process initiation, which slowed down the capillary action of the wick mesh. The effective thermal conductivity (K_{eff}) of the heat conduit was evaluated as follows:

$$K_{eff} = \frac{L_{eff}}{A_{cs}R_{th}} \quad \ldots (5)$$

$$L_{eff} = \frac{(L_{evapoator} + L_{condenser})}{2} + L_{adiabatic}[\text{m}] \quad \ldots (6)$$

where, L_{eff} is the effective length of the conduit. A_{cs} - cross-sectional area of the conduit, $R_{th}$is the thermal resistance of the heat conduit.

4.6 Validation of Experiments

Present experimental work was validated for the verification of the path and testing process; the primary index to validate with other experiments conducted in various conditions was total thermal resistance. This total thermal condition was compared with the 90° inclination and with active nanofluid of Al_2O_3working medium.

5. CONCLUSION

By incorporating Al_2O_3nanoparticles into DI water within a heat conduit featuring different inclinations, empirical investigations were effectively carried out on thermal performance within the conduit. The influence of gravity on heat transfer within the conduit was also investigated by exploring four unique tilt angles and different heat flux levels. The conclusions derived are:

- The heat conduit efficiency increased with the addition ofAl_2O_3nanoparticles in the base working fluid.
- The performance of the heat conduit was analyzed with respect to increasing heat flux and variations in the inclination angle.
- The HTC was increased by 5.68% to 21.7% based on the heat input applied to the evaporator section.
- The tilt angle had a significant impact on the heat resistance of the heat conduit when DI water was used as the base working fluid.
- With the increase in the inclination angle and the heat input, the heat resistance in the heat conduit decreased.
- Adding $Al_2O_3$to the base working fluid lowered the heat resistance of the heat conduit by 6.85% to 17.7%.
- The thermal efficiency of Al_2O_3nanofluids increased with the angle of inclination, but performance declined when the angle exceeded 60°.
- The Al_2O_3nanofluid exhibited considerable potential as a working fluid for heat conduits, particularly in thermosyphon applications without a wick, utilizing gravity for improved heat transfer performance.

REFERENCES

Bharathiraja, R., Ramkumar, T., Karthick L. and Mohanraj, M., Performance investigation on flat plate solar water collector using a hybrid nano-enhanced phase change material (PCM), *J. Energy Storage*, 86, 111163 (2024). https://doi.org/10.1016/j.est.2024.111163

Bumataria, R. and Chavda, N., Heat load and orientation impacts in cylindrical heat pipes using copper oxide, aluminium oxide, and zinc oxide nanofluids, *Int. J. Ambient. Energy*, 43(1), 6273–6283(2022). https://doi.org/10.1080/01430750.2021.2014957

Celata, G. P., Annibale, F., Mariani, A., Saraceno, L., Amato, R. and Bubbico, R., Heat Transfer in Water-Based SiC and TiO_2 Nanofluids, *Heat Transfer. Eng.*, 34(13), 1060–1072(2013). https://doi.org/10.1080/01457632.2013.763542

Do, K. H. and Jang, S. P., Effect of nanofluids on the thermal performance of a flat micro heat pipe with a rectangular grooved wick, *Int. J. Heat Mass Transfer*, 53(9–10), 2183–2192(2010). https://doi.org/10.1016/j.ijheatmasstransfer.2009.12.020

Kang, S. W., Wei, W. C., Tsai, S. H. and Yang, S. Y., Experimental investigation of silver nano-fluid on heat pipe thermal performance, *Appl. Therm. Eng.*, 26(17–18), 2377–2382(2006). https://doi.org/10.1016/j.applthermaleng.2006.02.020

Karthick, L., Senthil, M. V., Leon, J. L. S., Mallampati, M., Ahamed, M. and Loganathan, G. B., Energy performance of a compression refrigeration cycle using environment-friendly refrigerants, *Mater. Today: Proc.*, 66(3), 1519–1525(2022). https://doi.org/10.1016/j.matpr.2022.07.178

Karthick, L., Loganathan, G. B., Jagadish, C. A., Somasundaram, B., Kandavalli, S. R. and Chithambaranathan, P., Microhardness and Wear Rate Analysis on Laser Cladded Composites of AZ91D Alloy with SiC by Grey Technique, *Recent Adv. Mech. Eng.*, 2, 235–249 (2024). https://doi.org/10.1007/978-981-97-2249-5_21

Moraveji, K. and Razvarz, S., Experimental investigation of aluminum oxide nanofluid on heat pipe thermal performance, *Int. Commun. Heat. Mass Transfer*, 39(9), 1444–1448(2012). https://doi.org/10.1016/j.icheatmasstransfer.2012.07.024

Kim, H. D., Kim, J. and Kim, M. H., Experimental studies on CHF characteristics of nano-fluids at pool boiling, *Int. J. Multiphase. Flow*, 33(7), 691–706(2007). https://doi.org/10.1016/j.ijmultiphaseflow.2007.02.007

Kumaresan, G., Venkatachalapathy, S. and Asirvatham, L. G., Experimental investigation on enhancement in thermal characteristics of sintered wick heat pipe using CuO nanofluids, *Int. J. Heat Mass Transfer*, 72, 507–516(2014). https://doi.org/10.1016/j.ijheatmasstransfer.2014.01.029

Ma, H. B., Wilson, C., Borgmeyer, B., Park, K., Yu, Q., Choi, S. U. S. and Tirumala, M., Effect of nanofluid on the heat transport capability in an oscillating heat pipe, *Appl. Phys. Lett.*, 88(14), 143116(2006). https://doi.org/10.1063/1.2192971

Manay, E., Experimental investigation of mixed convection heat transfer of ferrite-based nanofluids in multiple microchannels, *Heat. Mass. Transfer.*, 55(2), 533–546(2019). https://doi.org/10.1007/s00231-018-2505-1

Mohanraj, M., Karthick, L. and Dhivagar, R., Performance and economic analysis of a heat pump water heater assisted regenerative solar still using latent heat storage, *Appl. Therm. Eng.*, 196, 117-263(2021). https://doi.org/10.1016/j.applthermaleng.2021.117263

Naphon, P., Assadamongkol, P. and Borirak, T., Experimental investigation of titanium nanofluids on the heat pipe thermal efficiency, *Int. Commun. Heat. Mass Transfer*, 35(10), 1316–1319(2008). https://doi.org/10.1016/j.icheatmasstransfer.2008.07.010

Pak, B. C. and Cho, Y. I., hydrodynamic and heat transfer study of dispersed fluids with submicron metallic oxide particles, *Exp. Heat Transfer*, 11(2), 151–170(1998). https://doi.org/10.1080/08916159808946559

Park, K. and Ma, H. B., Nanofluid Effect on the Heat Transport Capability in a Well-Balanced Oscillating Heat Pipe, *J. Thermophysics. Heat Transfer*, 21(2), 443–445(2007). https://doi.org/10.2514/1.22409

Razvarz, S. and Jafari, R., Experimental study of Al2O3 nanofluids on the thermal efficiency of curved heat pipe at different tilt angle, *J. Nanomater.*, *2018*(1), 1591247 (2018). https://doi.org/10.1155/2018/1591247

Senthilkumar, C., Krishnan, A. S. and Solomon, A. B., Effect of thin porous copper coating on the performance of wickless heat pipe with R134a as working fluid, *J. Therm. Anal. Calorim.*, 139(2), 963–973(2020). https://doi.org/10.1007/s10973-019-08176-x

Senthilkumar, R., Vaidyanathan, S. and Sivaraman, B., Effect of Inclination Angle in Heat Pipe Performance Using Copper Nanofluid, *Procedia Eng.*, 38, 3715–3721(2012). https://doi.org/10.1016/j.proeng.2012.06.427

Sharma, H. K., Kumar, S., Kumar, S. and Verma, S. K., Performance investigation of flat plate solar collector with nanoparticle enhanced integrated thermal energy storage system, *J. Energy Storage*, 55, 105681(2022). https://doi.org/10.1016/j.est.2022.105681

Shukla, K. N., Solomon, A. B., Pillai, B. C., Ruba Singh, B. J. and Saravana Kumar, S., Thermal performance of heat pipe with suspended nano-particles, *Heat Mass Transfer*, 48(11), 1913–1920(2012). https://doi.org/10.1007/s00231-012-1028-4

Vidhya, R., Balakrishnan, T. and Kumar, B. S., Experimental and theoretical investigation of heat transfer characteristics of cylindrical heat pipe using Al2O3–SiO2/W-EG hybrid nanofluids by RSM modeling approach, *J. Eng. Appl. Sci.*, 68(1), 32(2021). https://doi.org/10.1186/s44147-021-00034-8